

# Preparation of rod-shaped BaTiO<sub>3</sub> powder

YOSHIHIRO HAYASHI, TOSHIO KIMURA, TAKASHI YAMAGUCHI  
Faculty of Science and Technology, Keio University, Yokohama 223, Japan

Rod-shaped BaTiO<sub>3</sub> powder particles have been prepared from rod-shaped TiO<sub>2</sub> · nH<sub>2</sub>O and BaCO<sub>3</sub> in molten chloride. The morphology of BaTiO<sub>3</sub> particles was studied referring to the effects of the chemical species of the starting titanium compound, amount of chloride, particle size of the titanium compound and reaction conditions, and the preparation condition of rod-shaped BaTiO<sub>3</sub> has been determined: i.e., large TiO<sub>2</sub> · nH<sub>2</sub>O particles were heated at 700° C in molten salt with an equal amount of BaTiO<sub>3</sub>. This condition was effective in suppressing the formation of BaTiO<sub>3</sub> by a solution-precipitation process as well as the deformation of either TiO<sub>2</sub> · nH<sub>2</sub>O or BaTiO<sub>3</sub>, which are responsible for the formation of equiaxed BaTiO<sub>3</sub> particles. The obtained rod-shaped BaTiO<sub>3</sub> particles had a cubic symmetry. Electron diffraction analysis showed that the following topotactic relation is retained;

$$\langle 010 \rangle_{\text{potassium tetratitanate}} \parallel \langle 010 \rangle_{\text{hydrated titania}} \parallel \langle 100 \rangle_{\text{anatase}} \parallel \langle 100 \rangle_{\text{barium titanate}}$$

## 1. Introduction

Recent trends of ceramic powder preparation are toward either the preparation of ultrafine particles or the control of particle shape and agglomeration state [1, 2]. The particle shape is mainly determined by the formation process. As the conventional method by solid state reaction hardly controls the particle shape, novel techniques have been developed in which powders are prepared from a liquid or gas phase and nucleation and growth rates are controlled to develop a specific particle shape [3, 4]. These methods have been applied to simple oxides and a variety of powders with characteristic particle shapes have been prepared. Direct preparation of complex oxides is rather difficult and they are prepared via other compounds such as hydroxides and oxalates [5]. Conversion of these compounds into oxides by thermal decomposition causes agglomeration, the degree and strength of which depend on the precursor compound and decomposition condition.

One of the simple preparation methods of complex oxides is molten salt-synthesis, in which molten salts are used as solvent [6]. In this method, the control of the nucleation rate is rather difficult, because complex oxide particles are formed in the presence of solid reactant particles and the product nucleates usually on the reactant particles. Growth rate, on the other hand, can be controlled by selecting preparation conditions, such as salt species, heating temperature and duration. Because of the highly anisotropic nature of growth in molten salt, particle growth in molten salt tends to have a characteristic shape reflecting crystal symmetry [7]. Oxides with high symmetry such as cubic ferrites tend to be equiaxed, i.e. octahedron in the ferrite case. However, close examination of reaction mechanisms has enabled us to prepare plate-like ferrite particles [8].

This paper deals with the preparation of rod-shaped BaTiO<sub>3</sub> particles. Rod-shaped TiO<sub>2</sub> particles were heated with BaCO<sub>3</sub> in a NaCl-KCl mixed salt. The effects of various titanium starting sources and reaction conditions on the BaTiO<sub>3</sub> particle shape have been studied, and the mechanism of BaTiO<sub>3</sub> formation was discussed.

## 2. Experimental procedure

Rod-shaped TiO<sub>2</sub> was prepared from rod-shaped K<sub>2</sub>Ti<sub>4</sub>O<sub>9</sub>. Mixtures of K<sub>2</sub>CO<sub>3</sub>, TiO<sub>2</sub> and K<sub>2</sub>MoO<sub>4</sub>\* in a molar ratio of 6:24:70 were heated at 1000° C for 18 h [9], and then washed with hot water several times to remove K<sub>2</sub>MoO<sub>4</sub>. The main product was K<sub>2</sub>Ti<sub>4</sub>O<sub>9</sub> with a small amount of K<sub>2</sub>Ti<sub>6</sub>O<sub>13</sub> detected by X-ray diffraction analysis. The product was refluxed in boiling 1N HCl solution for 2 h to extract K<sub>2</sub>O. The resultant phase was TiO<sub>2</sub> · nH<sub>2</sub>O, which changes to anatase and rutile on heating for 1 h at 700° C and 1000° C, respectively [10]. Weight loss of TiO<sub>2</sub> · nH<sub>2</sub>O by a constant rate heating of 10° C min<sup>-1</sup> occurred between 100 and 500° C and was 7.6 wt % at 700° C, indicating that *n* is 0.38. Fig. 1 shows SEM photographs of K<sub>2</sub>Ti<sub>4</sub>O<sub>9</sub>, TiO<sub>2</sub> · nH<sub>2</sub>O and products obtained by heating TiO<sub>2</sub> · nH<sub>2</sub>O at 700 and 1000° C for 1 h. K<sub>2</sub>Ti<sub>4</sub>O<sub>9</sub> consisted of rod-shaped particles and this shape was preserved during the conversion to anatase. The transformation to rutile, however, changed the particle shape to spheroid.

Potassium tetratitanate, TiO<sub>2</sub> · nH<sub>2</sub>O or anatase, which was obtained by heating TiO<sub>2</sub> · nH<sub>2</sub>O at 700° C for 1 h, was wet-mixed with a stoichiometric quantity of BaCO<sub>3</sub> using a blender. The mixture was admixed with chloride flux (50 NaCl-50 KCl, m.p.: 650° C) and heated in a furnace kept at a desired temperature. The amount of the chloride mixture (designated by *W*) is defined by the weight ratio of the chloride to BaTiO<sub>3</sub>.

\*K<sub>2</sub>MoO<sub>4</sub> acts as a molten solvent to produce rod-shaped K<sub>2</sub>Ti<sub>4</sub>O<sub>9</sub>.

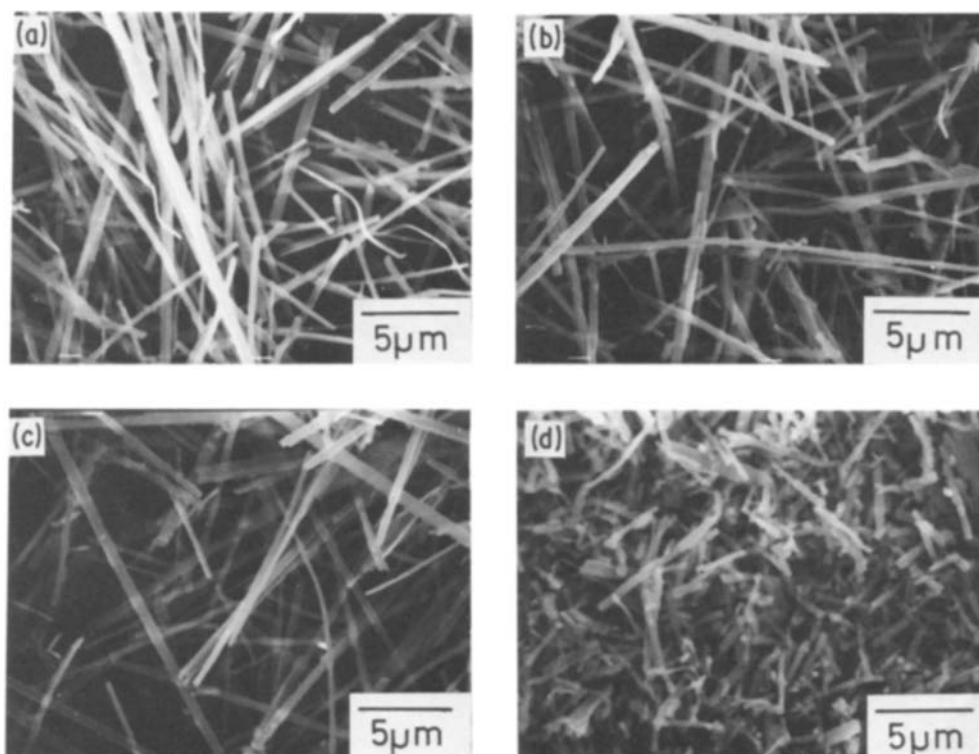


Figure 1 SEM photographs of (a)  $K_2Ti_4O_9$ , (b)  $TiO_2 \cdot nH_2O$  and products obtained by heating  $TiO_2 \cdot nH_2O$  for 1 h at (c)  $700^\circ C$  and (d)  $1000^\circ C$ .

After heating for a desired duration, the material was withdrawn from the furnace, cooled in air and washed with hot water several times. The resultant products were examined by X-ray diffraction analysis and scanning electron microscopy. The fractional reaction, was determined by the intensity ratio of the X-ray diffraction lines;

$$\alpha = I_{BT}/(I_{BT} + I_{BC}) \quad (1)$$

where  $I_{BT}$  and  $I_{BC}$  are peak areas of  $BaTiO_3$  (110) + (101) and of  $BaCO_3$  (111), respectively.

### 3. Results and discussion

#### 3.1. Preparation condition of rod-shaped $BaTiO_3$ particles

Potassium tetratitanate,  $TiO_2 \cdot nH_2O$  and anatase (shown in Fig. 1) were used as the titanium source and

heated with  $BaCO_3$  in the molten salt ( $W = 1.0$ ) at  $700^\circ C$  for 1 h. The product phase was always  $BaTiO_3$ , but the particle shape was dependent on the titanium source. Fig. 2 shows the particle shape and the fraction reacted. When  $K_2Ti_4O_9$  and anatase were used, the obtained  $BaTiO_3$  powders were the mixture of small equiaxed and large rod-shaped particles. The rod shape in the titanium source was preserved only when  $TiO_2 \cdot nH_2O$  was used. The  $BaTiO_3$  formation was completed by heating  $TiO_2 \cdot nH_2O$  for 1.5 h at  $700^\circ C$  in molten salt ( $W = 1.0$ ), but no significant change in particle shape was observed.

As the  $BaTiO_3$  powder composed of rod-shaped particles was obtained from  $TiO_2 \cdot nH_2O$ , the effects of reaction conditions on the shape of the resultant  $BaTiO_3$  were examined. Studies on the effect of salt on the reaction rate at  $700^\circ C$  showed that the salt accelerated the reaction regardless of the flux amount

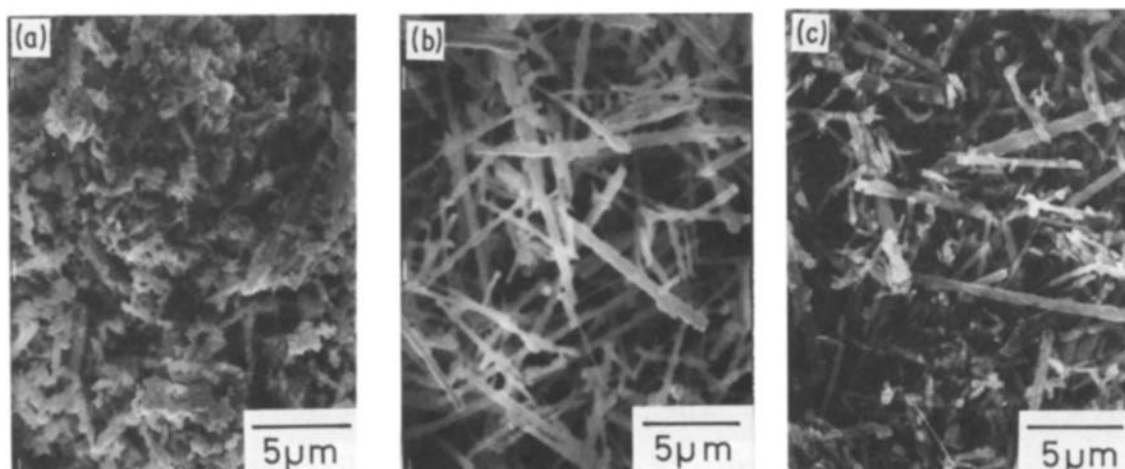


Figure 2 SEM photographs of reaction products between  $BaCO_3$  and (a)  $K_2Ti_4O_9$ , (b)  $TiO_2 \cdot nH_2O$  (c) anatase, heated at  $700^\circ C$  for 1 h ( $W = 1.0$ ). The fractional reactions ( $\alpha$ ) were 1.00, 0.90 and 0.94 respectively.

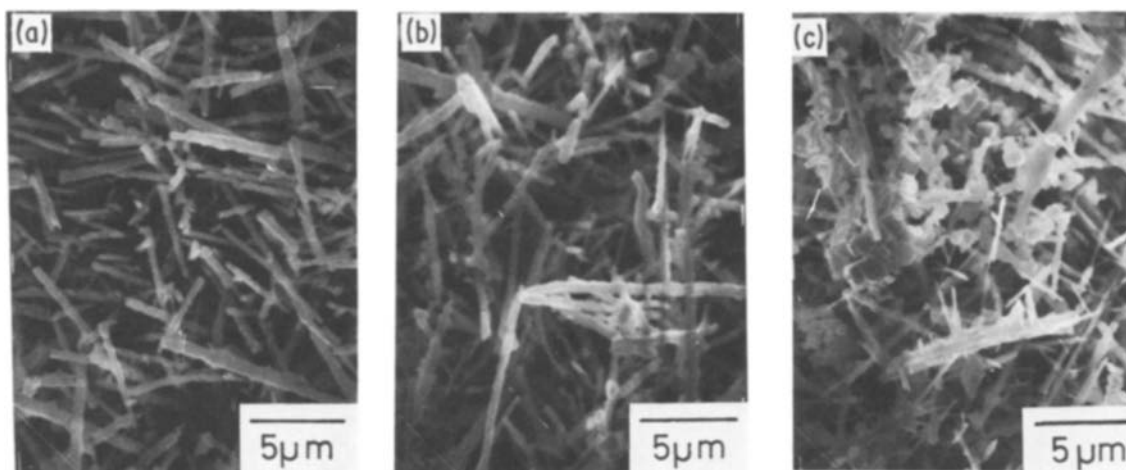


Figure 3 The effect of amount of salt on the product shape.  $\text{BaTiO}_3$  powders obtained by heating  $\text{TiO}_2 \cdot n\text{H}_2\text{O}$  at  $700^\circ\text{C}$  for 1 h with (a)  $W = 0.1$  ( $\alpha = 0.89$ ), (b)  $W = 2.0$  ( $\alpha = 0.91$ ) and (c)  $W = 4.0$  ( $\alpha = 0.89$ ).

employed. Fig. 3 shows the particle shape of the obtained products. Rod-shaped  $\text{BaTiO}_3$  powders were prepared at  $W$  between 0.1 and 2.0, and some large equiaxed particles were present with increasing amount of salt (Fig. 3c). Fig. 4 shows the effect of  $\text{TiO}_2 \cdot n\text{H}_2\text{O}$  particle size on the shape of  $\text{BaTiO}_3$  particles.  $\text{BaTiO}_3$  was obtained by heating small particles of  $\text{TiO}_2 \cdot n\text{H}_2\text{O}$  with  $\text{BaCO}_3$  at  $700^\circ\text{C}$  for 1 h ( $W = 1.0$ ). The resultant powder (Fig. 4b) contained equiaxed particles as well as rod-shaped ones. Fig. 5 shows the effect of heating temperature on the particle shape ( $W = 1.0$ ) of the product. The reaction was completed above  $800^\circ\text{C}$  by heating for 1 h. The increase in temperature promoted the formation of equiaxed  $\text{BaTiO}_3$  particles.

### 3.2. Reaction mechanisms in molten salt

The formation of rod-shaped  $\text{BaTiO}_3$  particles implies that barium ions diffuse through the  $\text{BaTiO}_3$  layers formed on the surface of titanium source particles. When no other reaction mechanisms are operative, rod-shaped  $\text{BaTiO}_3$  particles should be obtained as shown in Fig. 2b. First, we discussed the formation of equiaxed  $\text{BaTiO}_3$  particles at  $700^\circ\text{C}$  in the case using anatase and  $\text{K}_2\text{Ti}_4\text{O}_9$ . When rod-shaped  $\text{BaTiO}_3$  particles obtained at  $700^\circ\text{C}$  (Fig. 2b) were heated with molten salt at  $700^\circ\text{C}$  for another 1 h, no shape change occurred. This fact indicates that equiaxed  $\text{BaTiO}_3$  particles were formed before or during the reaction. The conver-

sion of anatase to rutile gave equiaxed  $\text{TiO}_2$  particles as shown in Fig. 1d. This conversion was accelerated when the anatase particles were heated in molten salt. Possibly, the equiaxed rutile particles were formed before the reaction with  $\text{BaCO}_3$ , resulting in the equiaxed  $\text{BaTiO}_3$  particles. The amount of rutile formed is probably much larger for anatase than  $\text{TiO}_2 \cdot n\text{H}_2\text{O}$  under the same temperature–time condition. The equiaxed particles in Fig. 2c may have been formed by “break-up” of the rod-shaped titanium source particles before the reaction. The “breaking up” of  $\text{K}_2\text{Ti}_4\text{O}_9$  is not probable, because the rod-shaped  $\text{K}_2\text{Ti}_4\text{O}_9$  alone is stable in molten salt. Thus, the equiaxed  $\text{BaTiO}_3$  particles in Fig. 2a would be formed during the reaction: i.e.,  $\text{K}_2\text{Ti}_4\text{O}_9$  and  $\text{BaCO}_3$  dissolve into molten salt and  $\text{BaTiO}_3$  precipitates out (solution–precipitation process). When the dissolution rate of the titanium source into the molten salt is smaller than that of  $\text{BaCO}_3$ , a  $\text{BaTiO}_3$  layer is formed on the surface of the titanium source particles and suppresses the dissolution of titanium. When the dissolution rate of titanium source particles is larger, on the other hand,  $\text{BaCO}_3$  reacts with dissolved titanium in the molten salt and no  $\text{BaTiO}_3$  layer is formed. The latter case should yield equiaxed, spherical or polyhedron particles, the faces of which are composed of low Miller indices, since the crystal structure of  $\text{BaTiO}_3$  at  $700^\circ\text{C}$  is cubic.

The amount of molten salt and particle size of

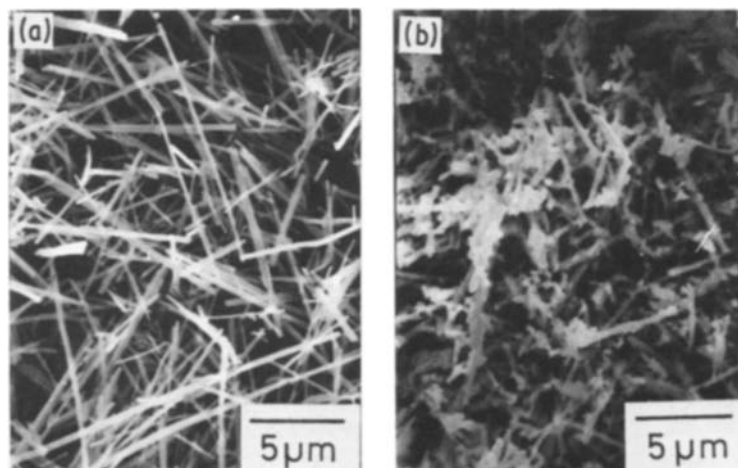


Figure 4 SEM photographs of (a) small starting particles of  $\text{TiO}_2 \cdot n\text{H}_2\text{O}$  and (b)  $\text{BaTiO}_3$  obtained by heating at  $700^\circ\text{C}$  for 1 h ( $W = 1.0$ ,  $\alpha = 0.96$ ).

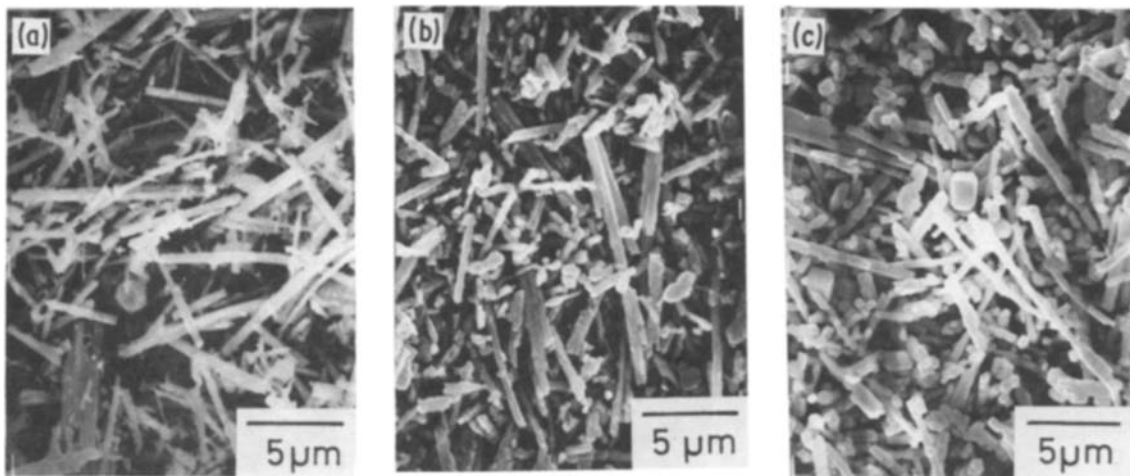


Figure 5 The effect of reaction temperature on the product shape, heated for 1 h ( $W = 1.0$ ) at (a) 700°C, (b) 800°C and (c) 900°C.

$\text{TiO}_2 \cdot n\text{H}_2\text{O}$  affect the relative dissolution rate of  $\text{TiO}_2 \cdot n\text{H}_2\text{O}$ . The larger amount of salt would require a longer time for saturation with the barium ion.  $\text{TiO}_2 \cdot n\text{H}_2\text{O}$  particles have a larger chance of dissolution, resulting in the increase in the amount of equiaxed particles (Fig. 3c). As small particles have a larger dissolution rate than larger ones, the equiaxed particles in Fig. 4b were formed probably by the solution-precipitation process.

Increasing the heating temperature also promoted the formation of equiaxed particles in the products. In order to understand the equiaxed particle formation at high reaction temperature, the particle shape change during 900°C-heating ( $W = 1.0$ ) was examined as shown in Fig. 6. The  $\text{BaTiO}_3$  formation was completed in 4 min at 900°C. The products obtained by heating within 4 min-heating consisted of only rod-shaped particles (Figs. 6a and b). Many equiaxed particles appeared in the 10 min-heated specimen (Fig. 6c). This fact indicates that rod-shaped  $\text{BaTiO}_3$  particles break up into equiaxed ones after being formed. Thus, at high heating temperatures the “break-up” of rod-shaped  $\text{BaTiO}_3$  particles could be a possible mechanism of equiaxed particle formation.

In summary, there are three possible mechanisms for the formation of equiaxed particles.

1. Rod-shaped titanium source particles break up into small equiaxed particles before reacting with  $\text{BaCO}_3$ . When a substance has a high crystal symmetry, the rod is not stable and breaks up into an equiaxed particle [11] as in the case of cylindrical void in sintered ceramics [12].

2.  $\text{TiO}_2 \cdot n\text{H}_2\text{O}$  and  $\text{BaCO}_3$  dissolve into molten salt and  $\text{BaTiO}_3$  precipitates out (solution-precipitation process).

3. Rod-shaped  $\text{BaTiO}_3$  particles once formed break up into small equiaxed particles by the same reason as in Mechanism (1).

### 3.3. Solid state method to prepare rod-shaped $\text{BaTiO}_3$ particles

The solid state reaction between  $\text{BaCO}_3$  and  $\text{TiO}_2$  proceeds by diffusion of barium ions, so that  $\text{BaTiO}_3$  particles with a shape similar to that of  $\text{TiO}_2$  are obtained [13]. It is possible to prepare the rod-shaped  $\text{BaTiO}_3$  particles by solid state reaction, if the same mechanism operates. The rod-shaped  $\text{TiO}_2 \cdot n\text{H}_2\text{O}$  particles were mixed with  $\text{BaCO}_3$  and heated at various temperatures for 1 h. The reaction was completed at 1000°C and the shape of the product is shown in Fig. 7. The  $\text{BaTiO}_3$  particles were rod-shaped and similar to those obtained in molten salt (Fig. 5a).

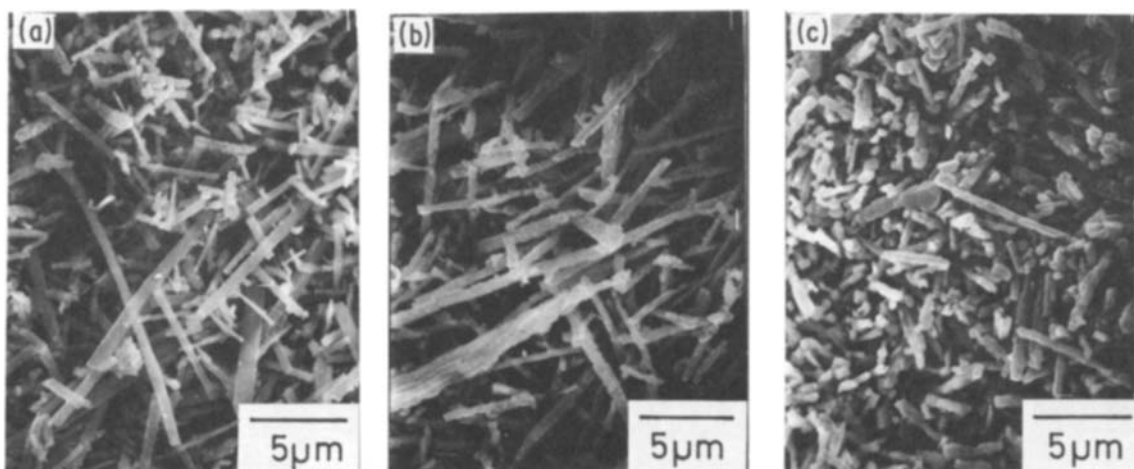


Figure 6 Particle shape changes during heating at 900°C in salt ( $W = 1.0$ ) for (a) 2 min ( $\alpha = 0.62$ ), (b) 4 min ( $\alpha = 1.00$ ) and (c) 10 min ( $\alpha = 1.00$ ). Samples in (a) was washed with 0.5 N HCl to remove unreacted  $\text{BaCO}_3$ .

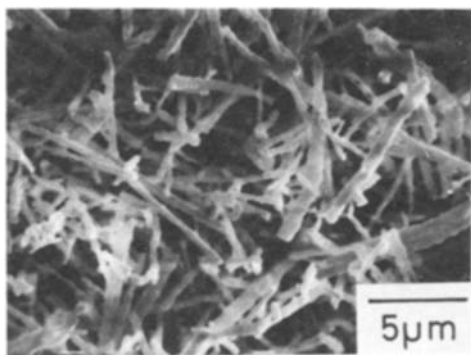


Figure 7 SEM of the product obtained by the conventional method.

Fig. 8 shows the particle size distribution of the product heated at 700°C for 1 h in molten salt (Fig. 5a) and that heated at 1000°C for 1 h by solid state reaction (Fig. 7). Particles were ultrasonically dispersed in water and the size was determined by the sedimentation method. The fraction of small sized particles obtained in molten salt is larger than that obtained by solid state reaction. As the particles are far from spherical, Stokes' law is not applicable and the obtained size does not correspond to the true particle size. However, this size distribution could reflect the size of the agglomerates, and consequently, the strength of the agglomerates in product powders. Thus, Fig. 8 implies that the powder obtained by solid state reaction contained larger and harder agglomerates. The reason why the powder prepared in the molten salt does not contain hard agglomerates is because the molten salt accelerates the reaction, lowering the reaction temperature. Moreover, the molten salt penetrates between the solid particles and prohibits the bonding of particles.

### 3.4. Characteristics of rod-shaped BaTiO<sub>3</sub> particles

In Section 3.2, we showed that the rod-shaped BaTiO<sub>3</sub> particles are unstable and change into equiaxed ones on prolonged heating at high temperature. Hence it is predicted that the tetragonality ( $c/a$ ) of rod-shaped BaTiO<sub>3</sub> powder is different from that of equiaxed

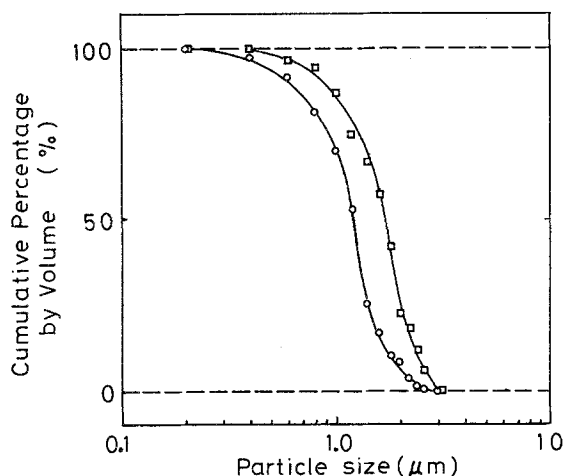


Figure 8 Particle size distribution of the rod-shaped BaTiO<sub>3</sub> powders obtained by heating for 1 h at (—○—) 700°C in salt ( $W = 1.0$ ) and (—□—) 1000°C without salt.

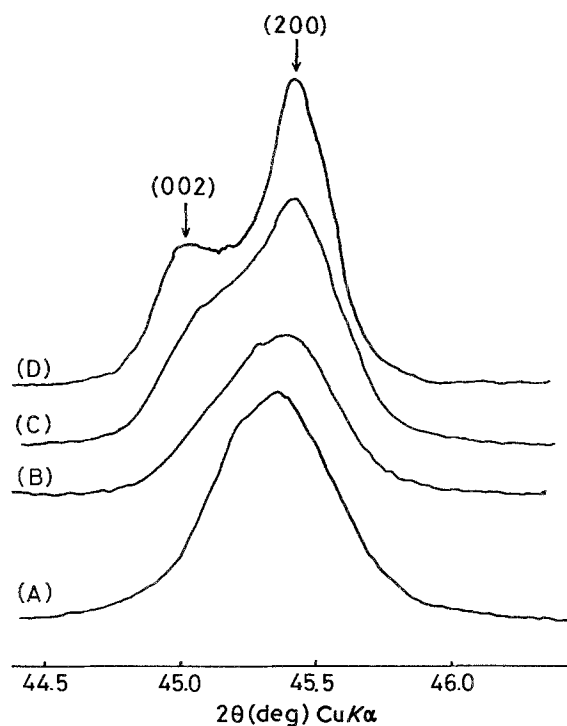


Figure 9 X-ray powder diffraction patterns showing tetragonal splitting of (200) and (002) lines. Profiles A, B and C correspond to diffraction lines of the BaTiO<sub>3</sub> powders shown in Figs. 5a, b and c. Profile D corresponds to the diffraction line of equiaxed BaTiO<sub>3</sub> powder with 0.8 μm diameter.

powder. Fig. 9 shows X-ray powder diffraction profiles of BaTiO<sub>3</sub> showing the effect of particle shape on the tetragonality. Profiles A, B and C correspond to the diffraction lines of BaTiO<sub>3</sub> powders shown in Figs. 5a, b and c, respectively. Profile D corresponds to the diffraction line of equiaxed BaTiO<sub>3</sub> powder with 0.8 μm-diameter, which was obtained from equiaxed TiO<sub>2</sub> ·  $n$ H<sub>2</sub>O powder. No tetragonal splitting was observed in Profile A. Tetragonal splitting becomes significant with increasing fraction of equiaxed particles in BaTiO<sub>3</sub> powders. These facts reveal that the tetragonal deformation is suppressed in rod-shaped BaTiO<sub>3</sub> particles. Fig. 10 shows the transmission electron microscopic photographs and electron diffraction patterns of rod-shaped TiO<sub>2</sub> ·  $n$ H<sub>2</sub>O and BaTiO<sub>3</sub> particles shown in Figs. 1b and 5a, respectively. The TEM observation indicates that a particle of BaTiO<sub>3</sub> is deformed. But the observed diffraction pattern of BaTiO<sub>3</sub> shows that the orientation is retained in the rod-shaped particle; the particle axis is parallel to the cubic  $a$ -axis. By electron diffraction analysis of rod-shaped titanium source particles reveals that the particle axes are parallel to the monoclinic  $b$ -axes [14] of K<sub>2</sub>Ti<sub>4</sub>O<sub>9</sub> and of TiO<sub>2</sub> ·  $n$ H<sub>2</sub>O and to the tetragonal  $a$ -axis of anatase. Thus, the orientation relation between titanium-source and BaTiO<sub>3</sub> particles is expressed as follows

$$\begin{aligned} \langle 010 \rangle_{\text{potassium tetratitanate}} &\parallel \langle 010 \rangle_{\text{hydrated titanate}} \\ &\parallel \langle 100 \rangle_{\text{anatase}} \parallel \langle 100 \rangle_{\text{barium titanate}} \end{aligned}$$

The structures of K<sub>2</sub>Ti<sub>4</sub>O<sub>9</sub>, TiO<sub>2</sub> ·  $n$ H<sub>2</sub>O, anatase and barium titanate contain TiO<sub>6</sub> octahedra [15, 16]. The observed directions of their particle axes coincide

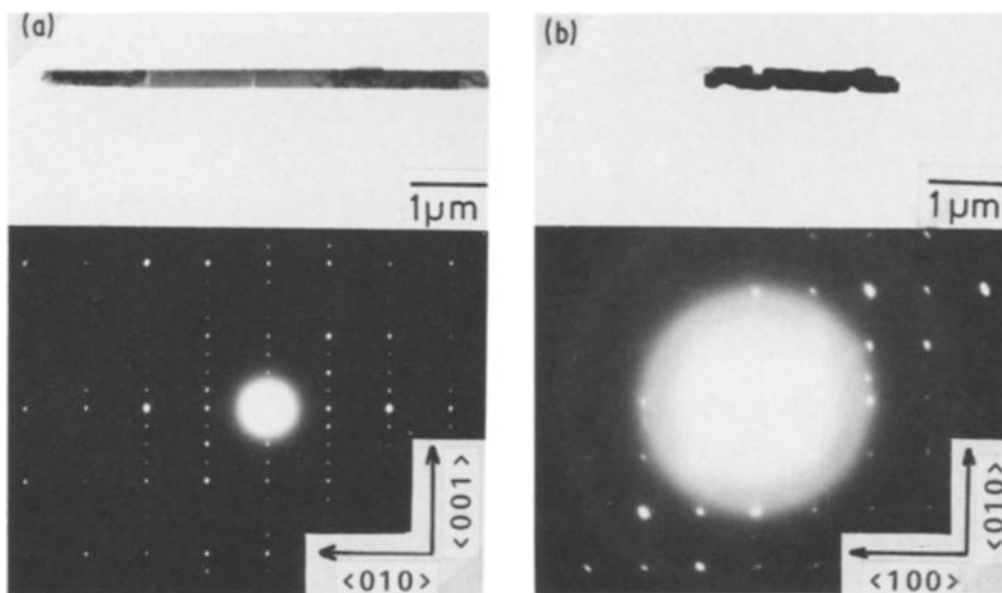


Figure 10 TEM and electron diffraction patterns of the rod-shaped (a)  $\text{TiO}_2 \cdot n\text{H}_2\text{O}$  and (b)  $\text{BaTiO}_3$  particles (shown in Fig. 1b and 5a.)

with the orientation of their  $\text{TiO}_6$  octahedra, implying that  $\text{BaTiO}_3$  formation takes place by topotactic reaction. Jonker [17] described that the tetragonal deformation is suppressed with decreasing crystallite size. The obtained rod-shaped  $\text{BaTiO}_3$  particle is probably polycrystalline containing very small crystallites. The very small crystallites in the obtained rod-shaped  $\text{BaTiO}_3$  particle might have been responsible for the suppression of cubic-tetragonal transition on cooling.

## References

1. E. A. BARRINGER and H. K. BOWEN, *J. Amer. Ceram. Soc.* **65**(12) (1982) C199.
2. W. H. RHODES, *ibid.* **64**(1) (1981) 19.
3. D. W. JOHNSON Jr, *Amer. Ceram. Soc. Bull.* **60**(2) (1981) 221.
4. E. MATIJEVIC, *Acc. Chem. Res.* **14**(1) (1981) 22.
5. K. S. MAZDIYASNI, *Amer. Ceram. Soc. Bull.* **63**(4) (1984) 591.
6. R. H. ARENDT, J. H. ROSOŁOWSKI and J. W. SZYMASZEK, *Mater. Res. Bull.* **14**(5) (1979) 703.
7. T. KIMURA and T. YAMAGUCHI, *Ceram. Internat.* **9**(1) (1983) 13.
8. T. KIMURA, T. TAKAHASHI and T. YAMAGUCHI, in *Ferrites*; Proceedings of the ICF3, edited by H. Watanabe, S. Iida and M. Sugimoto (Centre for Academic Publications, Tokyo, 1981) p. 27-29.
9. Y. FUJIKI and N. OHTA, *Yogyo-Kyokai-Shi* **88**(3) (1980) 111.
10. Y. FUJIKI, F. IZUMI, T. OHSAKA and M. WATANABE, *ibid.* **85**(10) (1977) 475.
11. F. A. NICHOLS, *J. Mater. Sci.* **11** (1976) 1077.
12. T. K. GUPTA, *J. Amer. Ceram. Soc.* **61**(5-6) (1978) 191.
13. Y. SUYAMA and A. KATO, *Bull. Chem. Soc. Jpn.* **50**(6) (1977) 1361.
14. H. IZAWA, S. KIKKAWA and M. KOIZUMI, *J. Phys. Chem.* **86** (1982) 5023.
15. N. OHTA and Y. FUJIKI, *Yogyo-Kyokai-Shi* **88**(1) (1980) 1.
16. Y. SUYAMA, Y. ODA and A. KATO, *Chem. Lett.* (1979) 987.
17. G. H. JONKER and W. NOORLANDER, in "Science of Ceramics" (Academic, New York, 1962) Vol. 1, pp. 255-64.

Received 25 March  
and accepted 2 April 1985